JCS ePress online publication date 22 February 2012

Reprogramming cell shape with laser nano-patterning

Timothée Vignaud[1], Rémi Galland[1], Qingzong Tseng[1], Laurent Blanchoin[1], Julien Colombelli[2]* and Manuel Théry[1]*

[1] Laboratoire de Physiologie Cellulaire et Végétale, Institut de Recherche en Technologies et Sciences pour le Vivant, CNRS/UJF/INRA/CEA, 17 rue des martyrs, 38054, Grenoble, France. [2] Advanced Digital Microscopy, Institute for Research in Biomedicine, Baldiri Reixac, 10, E-08028, Barcelona, Spain

*Correspondence: julien.colombelli@irbbarcelona.org, manuel.thery@cea.fr

Cell shape in vitro can be directed by geometrically-defined micropatterned adhesion substrates. However conventional methods are limited by the fixed micropattern design, which can not recapitulate the dynamic changes of the cell's microenvironment. Here, we manipulate the shape of living cells in real time by using scanned and tightly focused pulsed laser to introduce additional geometrically-defined adhesion sites. The sub-micrometer resolution of the laser patterning allowed us to identify the critical distances between cell adhesion sites required for cell shape extension and contraction. This easy-to-handle method allows a precise control of specific actin-based structures that regulate cell architecture. Actin filament bundles or branched meshworks were induced, displaced or removed in response to specific dynamic modifications of cell adhesion pattern. Isotropic branched actin meshworks could be forced to assemble locally new stress fibers and polarise in response to specific geometrical cues.

INTRODUCTION

The control of cell shape in vitro by the use of different designs of micropatterned substrates has been an insightful tool to investigate the fundamental rules of morphogenesis (Théry, 2010). This method has revealed that in addition to shape, cell behavior is also sensitive to the spatial distribution of its extracellular adhesions. Cell adhesion pattern has notably been shown to regulate cell architecture (Brock et al., 2003; Parker et al., 2002; Rossier et al., 2010; Théry et al., 2006a), polarity (Desai et al., 2009; James et al., 2008; Lombardi et al., 2011; Pitaval et al., 2010), migration (Doyle et al., 2009; Pouthas et al., 2008), division (Fink et al., 2011; Samora et al., 2011; Théry et al., 2007) and differentiation (Dupont et al., 2011; Kilian et al., 2010; McBeath et al., 2004).

The dynamic of cellular responses to changes in the microenvironment is a fundamental property of living systems that ensures the functional and mechanical coherence of tissues during development or renewal (Lu et al., 2011). However, the manipulation of changes in the microenvironment in vitro is limited with the use of conventional surface micropatterning methods because the design of the micropattern is fixed at the point of fabrication. Hence, the cellular responses to the geometry of these micropatterns can only be observed at steady-state; whereas cellular responses in real time to changes in the microenvironment cannot. This has been a major limitation in experimentally investigating the dynamic processes supporting cell and tissue morphogenesis.

Several approaches have been used to overcome this limitation and alter the adhesive environment surrounding the micropatterns on which living cells are attached (Nakanishi et al., 2008). Electric potential has been used to detach cell repellent coating, either by detaching micropatterned electroactive groups (Raghavan et al., 2010) or by desorbing coating above electrodes (Gabi et al., 2010; Kaji et al., 2006) thereby allowing constrained multicellular groups of cells on large micropatterns to invade specifically the activated regions. The minimum size of these regions was about 10 microns (Gabi et al., 2010). Alternatively, cell repellent moieties have been chemically linked to the silane coating by photo-cleavable groups so that they are released in response to UV light. Similarly, the loss of the cell repellent could either promote the local attachment of cells in suspension (Kikuchi et al., 2008b), trigger cell migration (Nakanishi et al., 2007) or promote the invasion of new areas by multicellular groups (Kikuchi et al., 2008a). With this method, substrate exposure to UV through a photomask placed in the optical plane of a microscope allowed the addition of new adhesive regions whose size could be as small as 5 microns (Nakanishi et al., 2007).

Here we have developed a simple method to ablate the cell repellent properties of the poly-ethylene glycol (PEG) coating in the vicinity of a live single cell already attached to a micropatterned substrate. The method uses a commercially available polymer to coat the cell culture substrate (polylysine-PEG) and pulsed-UV laser light to introduce additional adhesive regions. The manipulation of the adherent properties in the microenvironment of a single cell with sub-micrometer resolution enabled the precise control of intracellular architecture remodeling in real time.

RESULTS AND DISCUSSION

Laser patterning

Oxidation of a PEG layer on polystyrene (PS) coated glass is an efficient and versatile micropatterning method to accurately define geometries that can stereotypically direct cell adhesion and cell shape. Oxidation of PEG can be achieved by deep UV light exposure through a chromium mask (Azioune et al., 2010; Azioune et al., 2009). Deep UVs create ozone that oxidize the surface and allow protein adsorption (Mitchell et al., 2004). To create new micropatterned regions in the presence of living cells, we used a Q-switched laser producing 300 picoseconds pulses at 355nm and a high numerical aperture objective (Figure 1A). The accumulation of pulses energy in a highly confined volume induced the formation of a local plasma responsible for local oxidation and further destruction of irradiated materials (Colombelli et al., 2004; Colombelli et al., 2007; Pfleging et al., 2009; Vogel et al., 2005). We modulated the number and repetition rate of laser pulses as well as the laser power to control the size of individual spots. Laser patterning was conducted in the presence of fibrinogen-alexa546 to detect protein adsorption on exposed regions (Figure 1A). Surface modifications were also characterized by atomic force microscopy (AFM). Hexagonal arrays of spots separated by 160 nm were made using high or low laser beam power. High power beam did not allow homogeneous fibrinogen adsorption and resulted in a honeycomb like topography within the glass slide as seen by AFM with holes corresponding to laser spots (Figure 1B). Low power beam resulted in superficial (4nm) removal of the poly-lysine PEG and PS layers and efficient protein adsorption (Figure 1C). Therefore, these conditions were further adopted for live cell patterning in the rest of the study. However, the PS layer roughness induced a noisy AFM signal preventing the measurement of single laser spot width. Therefore, we decide to measure single spot size with higher power beam and a smaller polystyrene layer in order to induce detectable surface modification. In these conditions, the size of a single spot was 300 nm in diameter (Figure 1D). However it should be noted that the high power used in this procedure led to an overestimation of the actual method's spatial resolution. In the regular, low power, conditions used for live cell patterning, the spot size was probably smaller.

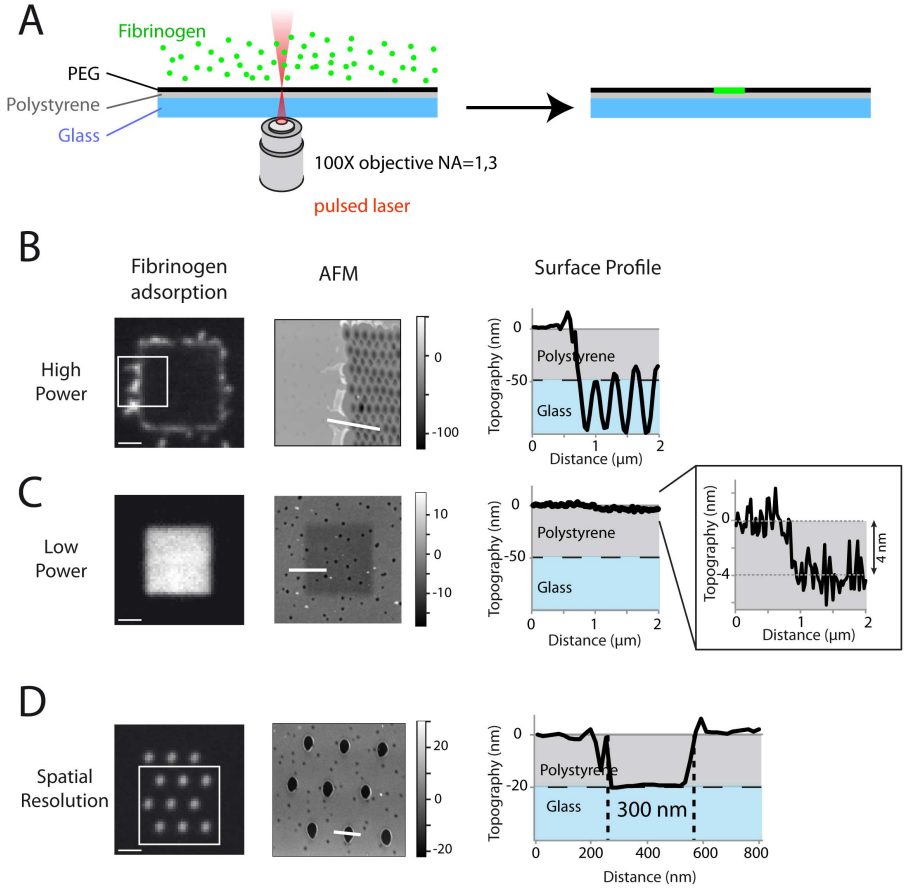

Figure 1 – Laser patterning. (A) Schematic representation of laser patterning. UV pulses locally remove the PEG coating and allow protein adsorbtion. (B) & (C) Arrays of spots separated by 160 nm were made using high (B) or low (C) laser beam power. (B) Fluorescence image of fibrinogen adsorption (left). High power beam did not allow homogeneous fibrinogen adsorption and resulted in a honeycomb like topography as seen by AFM (middle) with holes corresponding to laser spots. The surface profile along the line depicted in the AFM image was ploted (right). The polystyrene layer was removed and the glass coverslip was drilled. (C) Low power beam allow fibrinogen adsorption (left) and exhibit little surface modifications (middle). A 4 nm step was measured between non-exposed and exposed surfaces (right). (D) High power beam on thin polystyrene layer allowed fibrinogen adsorption (left) and resulted in holes reaching the glass surface (middle). The size of a single spot was 300 nm in diameter (right). Scale bars on fluorescence images represent 2 μm.

Critical geometrical determinants

Initial cell adhesion and early spreading, when cells just contacted the substrate, depend on the micro but also the nano-scale organization of adhesive ligands (Geiger et al., 2009). Integrins are transmembrane proteins connecting the ECM and the intra-cellular actin network. The engagement of actin filaments in between individual integrins participates to the clustering of integrins and the stimulation of membrane deformation and cell spreading. The distance between individual integrins needs to be smaller than 70 nm to allow actin filaments to connect their intracellular domains (Arnold et al., 2004). Integrin clusters must contain at least 4 integrin molecules within 60 nm to allow cell attachment (Schvartzman et al., 2011). The critical distance between these clusters that allow cell spreading depends on cluster size. It can be 25 μm on 9 μm2 adhesion spots, but is reduced to 5 μm on 0.1 μm2 spots (Lehnert et al., 2004). This suggests that, after the spreading phase, the subsequential cell extension and contraction onto the new adhesion sites could also depend on nano- and micro-scale organization of those adhesive sites.

The 300nm width of single spots (Figure 1D) allowed us to investigate the nano and micro-scale dependency of the cell extension and contraction phase. RPE1 cells were first plated on micropatterns made with classical deep-UV exposure through a photomask (Azioune et al., 2010; Azioune et al., 2009). They were allowed to spread and contract until their shape adopted the convex envelope of the micropattern (Rossier et al., 2010; Théry et al., 2006a). Then, using galvanometric mirrors, the laser beam was scanned on the substrate to draw the regions to be oxidized. This scanning method was a versatile and modulable way to design any kind of geometry anywhere around cells. Similar results could have been obtained also by moving the sample rather than the laser beam. Local PEG oxidation allowed cells to form new adhesions and to extend on the irradiated regions. The distance between individual adhesion spots could be varied up to the formation of a contiguous adhesive line (Figure 2A). Hence, this allowed us to identify the critical geometrical parameters allowing cell extension and contraction. Cells were attached to H shaped micropatterns and adopted a square shape of about 900 μm2. To test the requirements for the induction of a cell extension and the assembly of a new filament bundle, the two adhesive bars were extended at one side of the H with two new adhesive regions, made of parallel lines of adhesion spots. Cells did not extend on lines made of spots separated by 1900 nm (Figure 2B). Only a few cells could initiate extension on lines made of spots separated by 860 nm. More cells extended onto these lines when the inter-spot distance was reduced below 430nm (Figure 2C, E). However, the cell extensions could not generate a substantial contraction between the new adhesive regions, as revealed by the low values of the cell edge curvature radius (Théry et al., 2006a) (Figure 2C, E). Lines perpendicular to the longitudinal orientation of the H bar induced the same phenotypes (Figure S1). Interestingly, while cells could easily extend on dense square arrays of spots in which the inter-spot distance was 430nm, they could only generate a substantial contraction between the new adhesive regions when this distance was reduced to 160 nm, i.e. when the region was almost continuously adhesive (Figure 2D, E). These results showed that RPE1 cells required the adhesion spots to be separated by less than 430 nm in order to stabilize the new cell extension and a continuous adhesive region to generate a substantial contraction force. Previous reports showed that mouse melanoma cells can spread on similar arrays of 300nm-wide adhesion spots if their spacing is smaller than 5 microns (Lehnert et al., 2004). This suggests that the critical distance for extension and contraction in spread cells is one order of magnitude smaller than the critical distance for attachment and spreading.

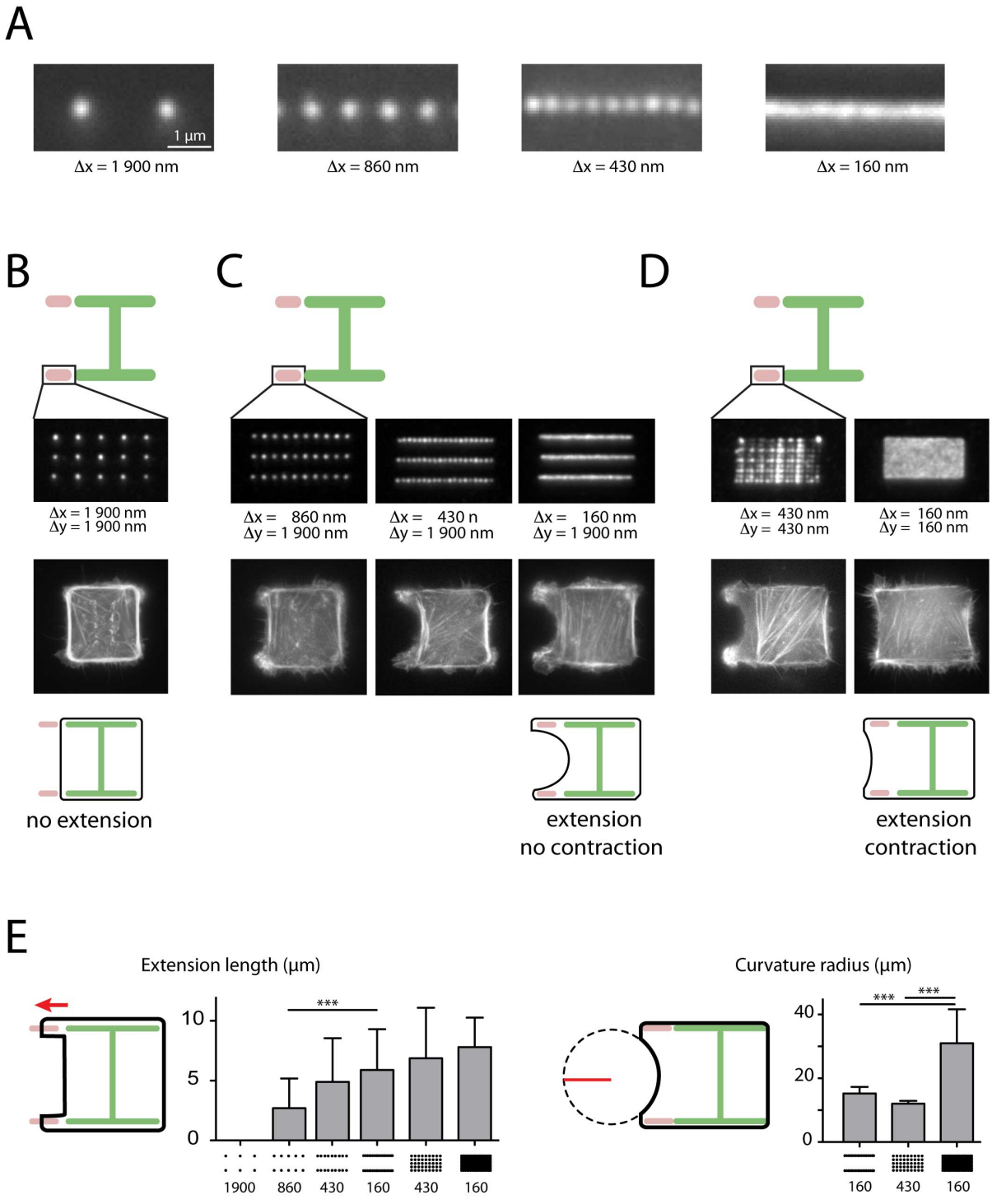

Figure 2 – Nano and microscale characteristics for cell extension and contraction. (A) Each spot corresponds to PEG-coated polystyrene exposure to 12 pulses during 20ms in the presence of fibrinogen-alexa546. Fibrinogen was immediately bound to the exposed regions. Drawing regions of interest in imaging software controlled displacements of galvanometric mirrors and laser positioning. Spot density along lines could be precisely controlled. (B-D) Cells were plated on H shaped micropatterns (green) and reprogrammed using laser patterning (red). The horizontal and vertical spacing between spots were varied from 1900 to 160 nm. New patterned regions are shown in the presence of fibrinogen-alexa546 for clarity (top images) but no fibrinogen was used during the experiments with cells. Images show the cells 3 hours after laser patterning. (B) Square arrays of dots with 1900 nm spacing did not allow cell extension on the newly patterned regions. (C) Newly patterned lines with a variety of spot spacing. Spots separated by 1900 nm promoted cell extension but not cell contraction. (D) square arrays of spots spaced with 430 nm allowed cell extension but not cell contraction while a 160nm spacing allowed both. (E) Left: mean measurement of cell extension length (n=18-20) on 10-micron long laser patterned regions corresponding to the above conditions. The number on the x-axis indicates the spot spacing. Right: mean measurement of free membrane curvature on horizontal lines with 160 nm spacing between the spots and on square arrays of spots separated by 430 nm or 160 nm. Measurements were performed only in cells forming full extensions on the two new patterned regions. The large curvature radius revealed a cell contraction between the new adhesive regions made of square arrays of spots separated by 160 nm. Error bars correspond to standard deviations, statistical test correspond to one-way ANOVA analyses.

Cell shape reprogramming

We could reprogram cell shape by adding the dense adhesive regions described above. For example, it was possible to remove the PEG from a region defined by a horizontal bar next to an apex of a triangularly-shaped cell constrained on a V shape (Figure 3A). After this ablation, the cell adhered also to this region and adopted a square shape (Figure 3B). Actin network reorganization during this cellular transformation was followed by monitoring Lifeact-GFP (Riedl et al., 2008). As the cell spread on the new bar, it formed many new actin cables, which connected the original and the new micropatterns. This showed that cells not only spread on to the laser-designed regions but also developed new internal cables during cell shape deformation from triangle to square (Figure 3B). The tension in these cables was probably required to support cell shape changes (Rossier et al., 2010; Théry et al., 2006a). We further investigated cell shape changes by adding two bars, above and below the original V shaped micropattern, and monitored cell shape extension in real time (Figure 3C and movie S1). As the cell shape changed, some peripheral actin cables disappeared (arrowhead in Figure 3C) while others were assembled (arrows in Figure 3C). This suggested that cell shape reprogramming was supported by complex remodeling of intracellular structures.

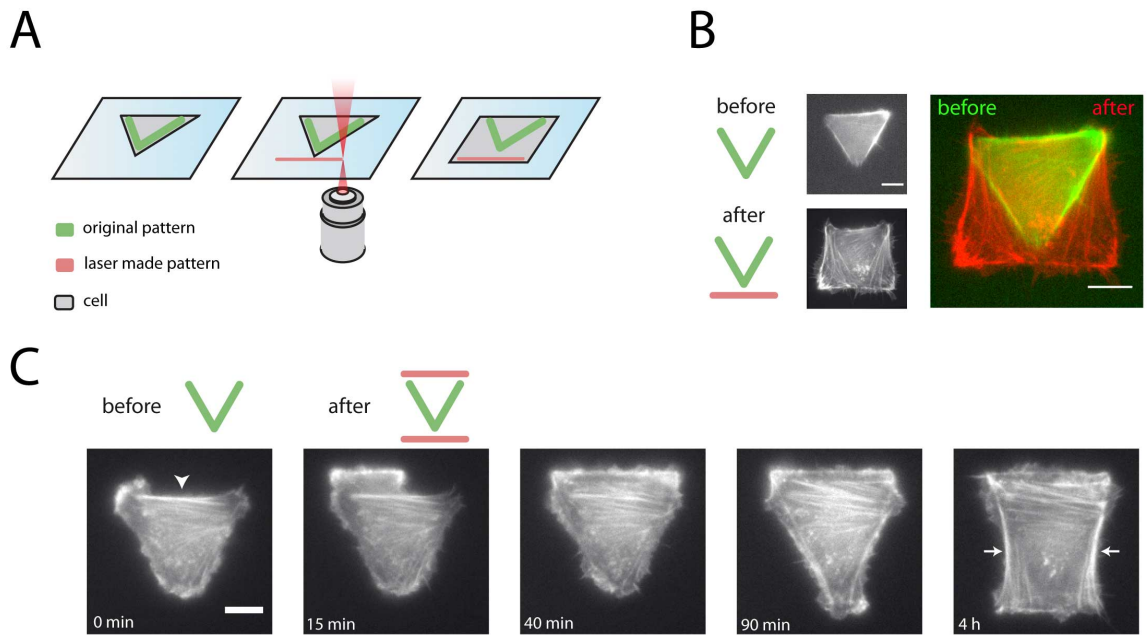

Figure 3 – Cell shape reprogramming. (A) Method description. Cells shape is first constrained on a classical micropattern (green). Pulsed laser is used to create new adhesive regions (red) in order to reprogram cell shape. (B) Example. A RPE1 cell expressing Lifeact-GFP is first constrained to have a triangular shape on a V shaped micropatten (top, green in the overlay) and then reprogrammed to become square (bottom, red in the overlay) by drawing a bar below the V shape with the laser. Scale bar is 10 microns. (C) Monitoring of cell shape changes. A triangular cell is first constrained on a V-shaped micropattern (green in the scheme) and reprogrammed to become rectangular by adding two horizontal bars above and below the original micropattern (red in the scheme). Cell shape changes were monitored in video-microscopy by observing Lifeact-GFP. Some actin filament bundles disappear (arrowhead) while others were assembled (arrows). Scale bar is 10 microns.

Controled actin network remodelling

Cell shape is supported by various structural elements made of actin filaments. They can be classified into branched meshworks and filament bundles (Michelot and Drubin, 2011). Both are highly dynamic and remodeled during cell shape changes (Rafelski and Theriot, 2004). We further tested whether laser-based patterning could be used to guide not only cell shape changes but also precise intracellular remodeling of these structural elements. Assembly of each structural element is dependent on local adhesion geometry (Brock et al., 2003; Parker et al., 2002; Théry et al., 2006a). When cultured on an H shaped micropattern, cells adopt a square shape. For a given cell, branched meshworks were established along the adhesive bars and actin bundles across the gaps. Each type of actin-based structures could be induced, displaced or removed during cell square shape transformation into a rectangle by adding new adhesive regions of defined geometries. Extending the length of the juxtaposed bars on one side promoted the displacement of the actin bundle so that it remained situated between the tips of the two bars (Figure 4A). Connecting the tips of two bars with a contiguous adhesive region favored actin bundle disassembly and the formation of a branched meshwork (Figure 4B). Adding two small bars perpendicular to one of the H bars induced formation of an additional peripheral actin bundle (Figure 4C). These results showed that in addition to controlling the global cell shape, the geometry and position of new adhesive regions could be used to finely control intracellular architecture remodeling.

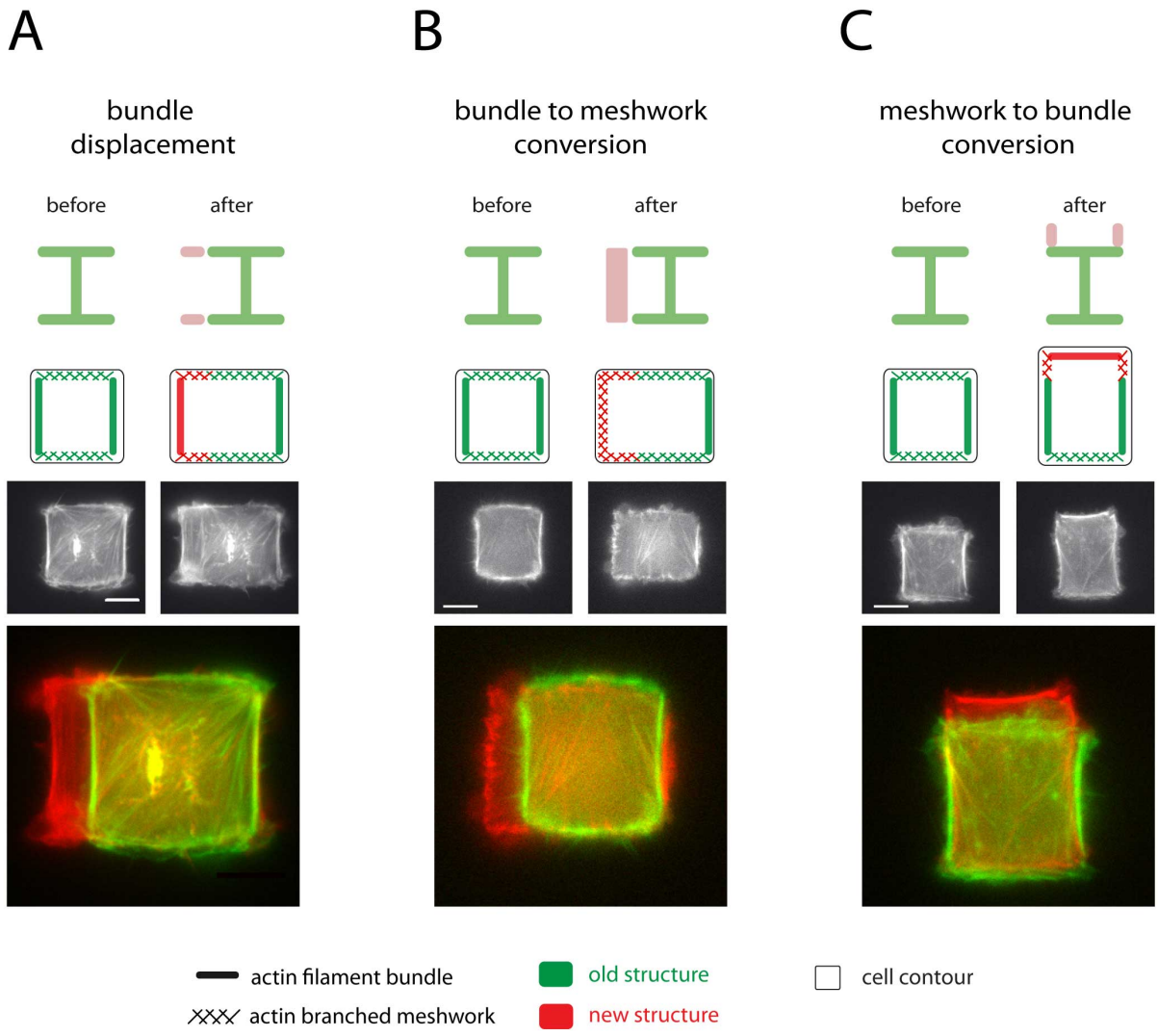

Figure 4 – Cell architecture manipulation. Cells were plated on H-shaped micropatterns (green in the upper schemes). Cell actin architecture was mainly composed of branched meshworks (thin crosses in the lower schemes) and filament bundles (thick bars). It was remodelled with laser patterning. Pre-existing structures are drawn in green in the lower schemes and shown in green in the images overlay, new ones are in red. Actin network architecture is revealed by the expression of Lifeact-GFP. Left images show the cell before and right images show the the cell 2 to 4 hours after laser patterning. Scale bars represent 10 microns. (A) Extending the two H bars (red in the upper schemes) in the same longitudinal direction as the original ones induced the disassembly of the pre-existing bundle and assembly of a new one connecting the tips of the new bars. (B) Connecting the tips of two H bars with a new perpendicular bar induced the disassembly of the pre-existing bundle and the formation of a branched meshwork on the new bar. (C) Adding two bars perpendicular and each at the tip of one of the H bars turned the branched meshwork along the original bar into a filament bundle in between the new bars.

In polarized cells, such as migrating cells or epithelial cells, the actin network is polarized into branched meshwork on one cell side and contractile stress fibers on the other. The precise sub-cellular location of stress fibers and acto-myosin contractile activity are critical to the determination of actin network polarity (Cramer, 2011) and internal cell polarity (Théry et al., 2006b). Live patterning could be used to precisely control and orient this actin network polarization step. A bar was added next to cells plated on a discoidal micropatterns (Figure 5A). Initially, cells actin networks did not displayed any significant polarized architecture. After live patterning, cells rapidly extended on the new bar and initiated the formation of contractile stress fibers along the edges connecting the disc and the tip of the bar (Figure 5B and movie S2). Upon completion of this extension and contraction phase, cells ended up with a highly asymmetric shape and polarized actin network.

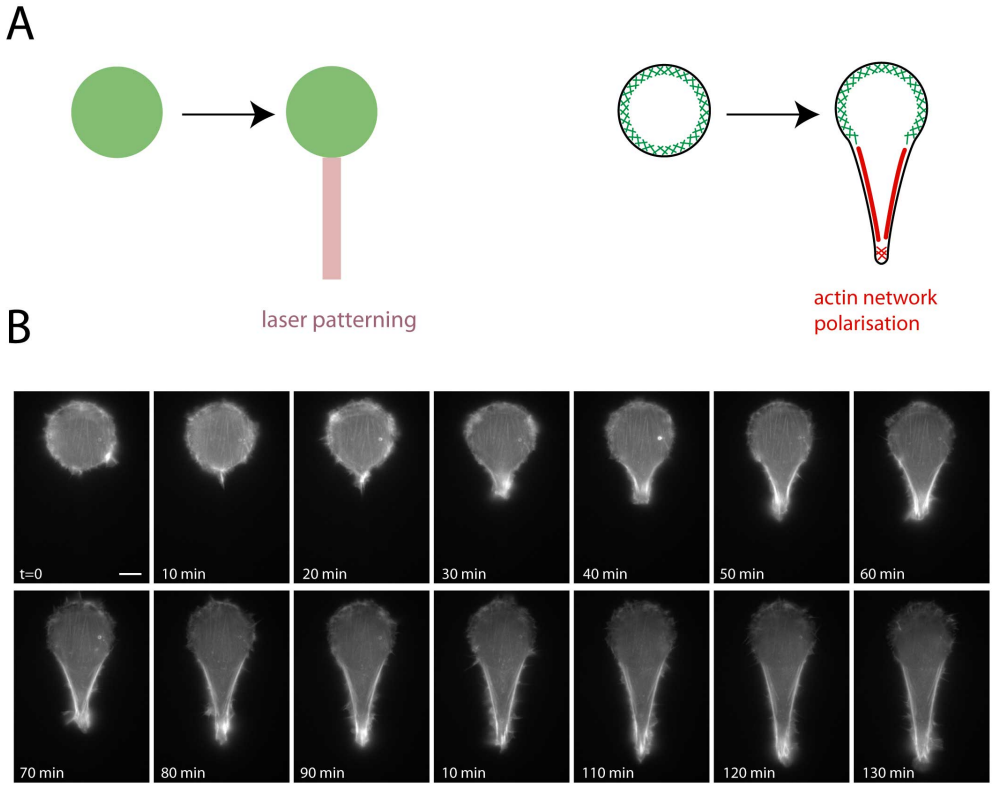

Figure 5 – Actin network polarisation. (A) Cells were plated on discoidal micropatterns (green). Cell actin architecture was initially mainly composed of an isotropic branched meshwork all along cell periphery (thin crosses). A bar perpendicular to disc border was added with laser patterning (red). Cells rapidly formed stress fibers connecting the disc and the bar tip (thick bars). Pre-existing structures are drawn in green and new ones are in red. (B) During this transformation, actin network architecture remodeling was monitored with Lifeact-GFP. Stress fibers were clearly visible after 30 minutes. They then get thicker and longer as cell extended on the bar. Scale bar represents 10 microns.

DISCUSSION

The laser patterning method we developed will found a broad range of applications in addition to the possibility to act on living cells. The non-specific action of this laser patterning method is a versatile way to design micropatterns on various surfaces. It does not require specific photo-activable substrates or photo-sensitive ligands. It simply ablates the protein repellent coating. Therefore it could be applied to any PEG coated surfaces. In addition it is a contact-less patterning method which therefore offers the possibility to design micropatterns on tridimensional substrates or in close microfluidic devices. Finally, the sequences of laser patterning and protein adsorption could be repeated at will in order to perform multi-protein patterning.

Here, we have demonstrated that this new and simple method for surface nano-patterning in live cell culture offers a precise control in real time of cell shape modifications and of intracellular architecture. This method should pave the way for further investigations of dynamic cellular responses to nano and micro-scale changes in the microenvironment. It also opens new possibilities to adapt “on the fly” the design of new geometrical constraints to the observed cell behavior. Therefore it will enable the fabrication of the micropatterned regions during the growth of multi-cellular groups. This will enable new insights into tissue engineering approach.

MATERIALS AND METHODS

Deep UV Patterning

Glass coverslip micro-patterning has been described elsewhere (Azioune et al., 2010). Briefly, coverslips were first spin-coated for 30 sec at 3000 rpm with adhesion promoter Ti-Prime (MicroChemicals, Germany), baked for 2 min at 120 °C and then spin-coated with 1% polystyrene solution (SIGMA, France) in toluene (SIGMA, France) at 1000 rpm for 30 s. Polystyrene coated coverslips were oxidized through oxygen plasma (FEMTO, Diener Electronics, France) 10s at 30W before incubating with 0.1mg/mL PLL-PEG (CYTOO, France) in 10mM HEPES pH=7.4 for 15min. After drying, coverslips were exposed to deep UV (UVO cleaner, Jelight, USA) through a photomask (TOPPAN, France) for 2min. Right after UV activation, coverslips were incubated with a 20 μg/mL of fibronectin (SIGMA) and 10 μg/mL Alexa-546 fibrinogen conjugate (Invitrogen) in Phosphate Buffer Solution (PBS) solution for 30 min. Coverslips were mounted in magnetic chambers (CYTOO, France) and washed 3 times with sterile PBS before plating cells.

Lifeact molecular cloning, lentiviral expression and cell transduction

LifeAct-mGFP plasmid were kindly provided by Wedlich-Soldner (Riedl et al., 2008). The lifeact-mGFP fragment was amplified by PCR using primers flanked with specific restriction enzyme site (namely EcoR1 and Not1). This fragment was subsequently cut and ligated with the pLVX lentiviral vector (Dupont et al., 632153, Clontech, Japan) which was also cut with corresponding restriction enzyme. The virus carrying the lifeact-mGFP were generated using the lenti-X packaging system (Dupont et al., 631247, Clontech, Japan).

hTERT-RPE1 cells (infinity telomerase-immortalised Retinal Pigment Epithelial human cell line) were subsequently infected with those virus followed by antibiotic selection, according to the manufacturer instructions (Clontech, Japan).

Cell culture

hTERT-RPE1 cells were cultured in DMEM F-12 (GIBCO) supplemented with 10 % Fetal Bovine Serum (A15-551, PAA, Germany), 50 Units/mL Penicillin and 50 μg/mL Streptomycin (15070-63, GIBCO). Cells were cultured in a 5% CO2 incubator at 37°C. Cells were trypsinised, centrifuged, resuspended in fresh medium and allow to spread on micro-pattern for 4 hours before the beginning of the experiment.

Laser patterning

Laser patterning was performed using of a Laser illuminator iLasPulse (ROPER SCIENTIFIC, France) set up on an inverted microscope (TE2000-E, Nikon, France). iLasPulse is a dual axis galvanometer based optical scanner that focalize the Laser beam on the sample (diffraction limited spot size) on the whole field of view of the camera. It includes a telescope to adjust Laser focalization with image focalization and a polarizer to control beam power. The laser used is a passively Q-switched laser (STV-E, TeamPhotonics, France) that produce 300 picoseconds pulses at 355nm (Energy/Pulse 1.2μJ /Peak Power 4 kW/ Variable Repetition rate 0.01 to 2 KHz / Average power ≤2.4mW). Laser displacement, exposure time and repetition rate are controlled using Metamorph® software (Universal Imaging Corporation). The objective used is a 100x CFI S Fluor oil objective (MRH02900, Nikon, France). The area to pattern was filled with different density of spot. Each spot was exposed for 20 ms at a repetition rate of 600 Hz. The polarizer was set to have an energy per pulse of 300 nJ.

To vizualize the patterned zone, a polystyrene/PLL-PEG treated coverslip (see « Deep UV Patterning » section) without cell was mounted in a magnetic chamber. This chamber was filled with a 20 µg/mL fibronectin (, SIGMA, France) and 10 µg/mL fluorescent fibrinogen conjugate (Invitrogen, France) PBS solution. Laser patterning was then conducted as described above and protein adsorption was allowed for 30 minutes. Coverslips were rinced with PBS and fluorescent images were then taken through a 100x UplanSApo oil objective (Olympus, France) using an olympus BX61 microscope (Olympus, France) and a CoolSNAP HQ2 camera (Photometrics, France).

Image acquisition

Magnetic chambers containing the coverslips and filled with cell culture medium were put on the microscope (TE2000-E, Nikon, France) in a stage incubator system at 37°C and 5% CO2 (Chamlide WP, Live Cell Instruments, Korea). Epifluorescence images of cells were acquired through a 100x CFI Plan Fluor oil objective or 60x CFI Apo TIRF oil

objective (MRH02900 and MBH76162 respectively, Nikon, France) and a QUANTEM:512SC cooled EMCCD camera (Photometrics). The whole system is controlled by Metamorph® software (Universal Imaging Corporation).

Cell extension and membrane curvature measurements

Extension and curvature measurements were performed using ImageJ software.

For extension measurement, the distance between the border of the initial pattern and the border of the cell extended on the new pattern was measured. Two measures were performed for each cell (one for each extension zone).

For curvature measurements, a circle was manually drawn along the unattached edge of the cell joining the two new adherent zone and the radius of the circle was measured automatically. Only cells that have extended on the two bar were measured.

All the measurement series were compared using a one-way Anova comparison test. Means were considered as significantly different when the P value was below 0.05 (*: $P < 0.05$, **: $P < 0.01$, ***: $P < 0.001$, **** : $P<0.0001$).

Atomic Force Microscopy

Laser-made miropatterns were observed and quantified in Atomic Force Microscopy (AFM) to see the topographical effect induced by the procedure.

AFM was performed on a 5500 LS AFM stage (Agilent) or a DI 3100 AFM stage (Veeco). Coverslips were attached to a glass slide and mounted in the AFM. Ambient tapping mode imaging was performed using a NSC19 cantilever (Mikromasch). Scan parameters were optimized to minimize the difference between the set point and the amplitude of the free cantilever while maintaining a stable image.

To estimate the size of a single spot, a polystyrene/PLL-PEG treated coverslip (see « Deep UV Patterning » section) without cell was mounted in a magnetic chamber. As the single spot margins could not be clearly seen in AFM due to the small size of the topographical step (8 nm) compared to the polystyrene surface roughness (see Figure 1), the laser beam intensity was increased in order to make small holes in the polystyrene layer. Therefore the width of 300nm is an overestimation of the actual spot we used in the experiments in the presence of cells.

ACKNOWLEDGMENT

We thank David Peyrade and Patrice Baldeck for technical help during preliminary experiments and Simon Le Denmat for AFM analyses. This work was supported by grants from Agence National pour la Recherche (ANR-PCV08-322457, ANR-08-JC-0103 to MT), and two PhD fellowships from the IRTELIS program of the CEA to TV and QT and a Post-doctoral fellowship from the Chimtronique program of the CEA to RG.

REFERENCES

Arnold, M., Cavalcanti-Adam, E. A., Glass, R., Blummel, J., Eck, W., Kantlehner, M., Kessler, H. and Spatz, J. P. (2004). Activation of integrin function by nanopatterned adhesive interfaces. *Chemphyschem* **5**, 383-388.

Azioune, A., Carpi, N., Tseng, Q., Thery, M. and Piel, M. (2010). Protein micropatterns: A direct printing protocol using deep UVs. *Methods Cell Biol* **97**, 133-146.

Azioune, A., Storch, M., Bornens, M., Thery, M. and Piel, M. (2009). Simple and rapid process for single cell micro-patterning. *Lab Chip* **9**, 1640-1642.

Brock, A., Chang, E., Ho, C. C., LeDuc, P., Jiang, X., Whitesides, G. M. and Ingber, D. E. (2003). Geometric determinants of directional cell motility revealed using microcontact printing. *Langmuir* **19**, 1611-1617.

Colombelli, J., Grill, S. W. and Stelzer, E. H. K. (2004). Ultraviolet diffraction limited nanosurgery of live biological tissues. *Review of Scientific Instruments* **75**, 472-478.

Colombelli, J., Reynaud, E. G. and Stelzer, E. H. (2007). Investigating relaxation processes in cells and developing organisms: from cell ablation to cytoskeleton nanosurgery. *Methods Cell Biol* **82**, 267-291.

Cramer, L. P. (2011). Forming the cell rear first: breaking cell symmetry to trigger directed cell migration. *Nat Cell Biol* **12**, 628-632.

Desai, R. A., Gao, L., Raghavan, S., Liu, W. F. and Chen, C. S. (2009). Cell polarity triggered by cell-cell adhesion via E-cadherin. *J Cell Sci* **122**, 905-911.

Doyle, A. D., Wang, F. W., Matsumoto, K. and Yamada, K. M. (2009). One-dimensional topography underlies three-dimensional fibrillar cell migration. *J Cell Biol* **184**, 481-490.

Dupont, S., Morsut, L., Aragona, M., Enzo, E., Giulitti, S., Cordenonsi, M., Zanconato, F., Le Digabel, J., Forcato, M., Bicciato, S. et al. (2011). Role of YAP/TAZ in mechanotransduction. *Nature* **474**, 179-183.

Fink, J., Carpi, N., Betz, T., Betard, A., Chebah, M., Azioune, A., Bornens, M., Sykes, C., Fetler, L., Cuvelier, D. et al. (2011). External forces control mitotic spindle positioning. *Nat Cell Biol* **13**, 771-778.

Gabi, M., Larmagnac, A., Schulte, P. and Voros, J. (2010). Electrically controlling cell adhesion, growth and migration. *Colloids and Surfaces B-Biointerfaces* **79**, 365-371.

Geiger, B., Spatz, J. P. and Bershadsky, A. D. (2009). Environmental sensing through focal adhesions. *Nat Rev Mol Cell Biol* **10**, 21-33.

James, J., Goluch, E. D., Hu, H., Liu, C. and Mrksich, M. (2008). Subcellular curvature at the perimeter of micropatterned cells influences lamellipodial distribution and cell polarity. *Cell Motil Cytoskeleton* **65**, 841-852.

Kaji, H., Kawashima, T. and Nishizawa, M. (2006). Patterning cellular motility using an electrochemical technique and a geometrically confined environment. *Langmuir* **22**, 10784-10787.

Kikuchi, Y., Nakanishi, J., Nakayama, H., Shimizu, T., Yoshino, Y., Yamaguchi, K., Yoshida, Y. and Horiike, Y. (2008a). Grafting Poly(ethylene glycol) to a Glass Surface via a Photocleavable Linker for Light-induced Cell Micropatterning and Cell Proliferation Control. *Chemistry Letters* **37**, 1062-1063.

Kikuchi, Y., Nakanishi, J., Shimizu, T., Nakayama, H., Inoue, S., Yamaguchi, K., Iwai, H., Yoshida, Y., Horiike, Y., Takarada, T. et al. (2008b). Arraying heterotypic single cells on photoactivatable cell-culturing substrates. *Langmuir* **24**, 13084-13095.

Kilian, K. A., Bugarija, B., Lahn, B. T. and Mrksich, M. (2010). Geometric cues for directing the differentiation of mesenchymal stem cells. *Proc Natl Acad Sci U S A* **107**, 4872-4877.

Lehnert, D., Wehrle-Haller, B., David, C., Weiland, U., Ballestrem, C., Imhof, B. A. and Bastmeyer, M. (2004). Cell behaviour on micropatterned substrata: limits of extracellular matrix geometry for spreading and adhesion. *J Cell Sci* **117**, 41-52.

Lombardi, M. L., Jaalouk, D. E., Shanahan, C. M., Burke, B., Roux, K. J. and Lammerding, J. (2011). The interaction between nesprins and sun proteins at the nuclear envelope is critical for force transmission between the nucleus and cytoskeleton. *J Biol Chem* **286**, 26743-26753.

Lu, P., Takai, K., Weaver, V. M. and Werb, Z. (2011). Extracellular Matrix Degradation and Remodeling in Development and Disease. *Cold Spring Harb Perspect Biol* **Epub ahead of print**.

McBeath, R., Pirone, D. M., Nelson, C. M., Bhadriraju, K. and Chen, C. S. (2004). Cell shape, cytoskeletal tension, and RhoA regulate stem cell lineage commitment. *Dev Cell* **6**, 483-495.

Michelot, A. and Drubin, D. G. (2011). Building distinct actin filament networks in a common cytoplasm. *Curr Biol* **21**, R560-R56 9.

Mitchell, S. A., Poulsson, A. H., Davidson, M. R., Emmison, N., Shard, A. G. and Bradley, R. H. (2004). Cellular attachment and spatial control of cells using micro-patterned ultra-violet/ozone treatment in serum enriched media. *Biomaterials* **25**, 4079-4086.

Nakanishi, J., Kikuchi, Y., Inoue, S., Yamaguchi, K., Takarada, T. and Maeda, M. (2007). Spatiotemporal control of migration of single cells on a photoactivatable cell microarray. *J Am Chem Soc* **129**, 6694-6695.

Nakanishi, J., Takarada, T., Yamaguchi, K. and Maeda, M. (2008). Recent advances in cell micropatterning techniques for bioanalytical and biomedical sciences. *Analytical Sciences* **24**, 67-72.

Parker, K. K., Brock, A. L., Brangwynne, C., Mannix, R. J., Wang, N., Ostuni, E., Geisse, N. A., Adams, J. C., Whitesides, G. M. and Ingber, D. E. (2002). Directional control of lamellipodia extension by constraining cell shape and orienting cell tractional forces. *Faseb J* **16**, 1195-1204.

Pfleging, W., Torge, M., Bruns, M., Trouillet, V., Welle, A. and Wilson, S. (2009). Laser- and UV-assisted modification of polystyrene surfaces for control of protein adsorption and cell adhesion. *Applied Surface Science* **255**, 5453-5457.

Pitaval, A., Tseng, Q., Bornens, M. and Théry, M. (2010). Cell shape and contractility regulate ciliogenesis in cell cycle arrested cells. *The Journal of Cell Biology* **191**, 303-312.

Pouthas, F., Girard, P., Lecaudey, V., Ly, T. B., Gilmour, D., Boulin, C., Pepperkok, R. and Reynaud, E. G. (2008). In migrating cells, the Golgi complex and the position of the centrosome depend on geometrical constraints of the substratum. *J Cell Sci* **121**, 2406-2414.

Rafelski, S. M. and Theriot, J. A. (2004). Crawling toward a unified model of cell mobility: spatial and temporal regulation of actin dynamics. *Annu Rev Biochem* **73**, 209-239.

Raghavan, S., Desai, R. A., Kwon, Y., Mrksich, M. and Chen, C. S. (2010). Micropatterned dynamically adhesive substrates for cell migration. *Langmuir* **26**, 17733-17738.

Riedl, J., Crevenna, A. H., Kessenbrock, K., Yu, J. H., Neukirchen, D., Bista, M., Bradke, F., Jenne, D., Holak, T. A., Werb, Z. et al. (2008). Lifeact: a versatile marker to visualize F-actin. *Nat Methods* **5**, 605-607.

Rossier, O. M., Gauthier, N., Biais, N., Vonnegut, W., Fardin, M. A., Avigan, P., Heller, E. R., Mathur, A., Ghassemi, S., Koeckert, M. S. et al. (2010). Force generated by actomyosin contraction builds bridges between adhesive contacts. *EMBO J* **29**, 1055-1068.

Samora, C. P., Mogessie, B., Conway, L., Ross, J. L., Straube, A. and McAinsh, A. D. (2011). MAP4 and CLASP1 operate as a safety mechanism to maintain a stable spindle position in mitosis. *Nat Cell Biol* **13**, 1040-1050.

Schvartzman, M., Palma, M., Sable, J., Abramson, J., Hu, X., Sheetz, M. P. and Wind, S. J. (2011). Nanolithographic control of the spatial organization of cellular adhesion receptors at the single-molecule level. *Nano Lett* **11**, 1306-1312.

Théry, M. (2010). Micropatterning as a tool to decipher cell morphogenesis and functions. *J Cell Sci* **123**, 4201-4213.

Théry, M., Jimenez-Dalmaroni, A., Racine, V., Bornens, M. and Julicher, F. (2007). Experimental and theoretical study of mitotic spindle orientation. *Nature* **447**, 493-496.

Théry, M., Pepin, A., Dressaire, E., Chen, Y. and Bornens, M. (2006a). Cell distribution of stress fibres in response to the geometry of the adhesive environment. *Cell Motil Cytoskeleton* **63**, 341-355.

Théry, M., Racine, V., Piel, M., Pepin, A., Dimitrov, A., Chen, Y., Sibarita, J. B. and Bornens, M. (2006b). Anisotropy of cell adhesive microenvironment governs cell internal organization and orientation of polarity. *Proc Natl Acad Sci U S A* **103**, 19771-19776.

Vogel, A., Noack, J., Huttman, G. and Paltauf, G. (2005). Mechanisms of femtosecond laser nanosurgery of cells and tissues. *Applied Physics B-Lasers and Optics* **81**, 1015-1047.